Geophys. J. Int. (2004) **159,** 104–116 doi: 10.1111/j.1365-246X.2004.02370.x

Magnetic properties of the profiles of polluted and non-polluted soils. A case study from Ukraine

Maria Jeleńska,[1] Agata Hasso-Agopsowicz,[1] Barbara Kopcewicz,[1] Anatoliy Sukhorada,[2] Ksenija Tyamina,[2] Magdalena Kądziałko-Hofmokl[1] and Zhanna Matviishina[3]

[1]*Institute of Geophysics, Polish Academy of Sciences, Ks. Janusza* 64, 01-452 *Warsaw, Poland. E-mail: bogna@igf.edu.pl*
[2]*National Taras Shevchenko University of Kyiv, Geological Faculty,* 90 *Vasylkovska St.,* 03022 *Kyiv, Ukraine*
[3]*Institute of Geography, National Academy of Sciences Ukraine* 44 *Volodymyrska St.* 01034 *Kyiv, Ukraine*

Accepted 2004 May 24. Received 2004 May 24; in original form 2003 November 10

SUMMARY

This report deals with the preliminary study of the magnetic properties of the chernozem depth profiles from polluted and non-polluted areas situated in the Volnovaha–Mariupol agro-soil region in southeast Ukraine. The profiles of soil for study were taken from the chernozem virgin land of the Homutovski steppe and from the nearby polluted area of Mariupol belonging to the Dniprovsko–Donetskij industrial region. The magnetic mineralogy and magnetic properties were examined along the profiles to determine the vertical structure of the non-polluted soil and to find differences caused by pollution. The soil from the non-polluted area is characterized by maghemite and haematite content. Magnetite is present in the topsoil of profiles from the polluted area of Mariupol. Blocking temperatures increase with depth in all profiles, becoming close to the temperature characteristic for haematite. Hysteresis parameters show that the deep soil is characterized by higher coercivity and coercivity of remanence values and lower saturation isothermal remanent magnetization and saturation magnetization values than the respective parameters in the topsoil. The grain size of magnetic minerals also changes with depth, becoming larger for deeper horizons. The surface values of susceptibility, saturation magnetization, saturation isothermal remanent magnetization and anhysteretic remanent magnetization for the polluted profiles from Mariupol show enhancement in relation to the values for the Homutowski steppe as a result of contamination by magnetite and haematite. However, starting from a depth of approximately 80–100 cm, the magnetic parameters approach the same values. This suggests that in deep horizons a lithogenic contribution prevails, similar for both areas.

Key words: chernozem, magnetic mineralogy, magnetic properties, pollution, Ukraine.

1 INTRODUCTION

In recent years studies of magnetic characteristics have become one of the most important methods in investigations of anthropogenic impact on soils (Maher 1986; Maher *et al.* 1999; Petrovsky & Ellwood 1999). In this paper magnetic methods are applied to polluted and non-polluted soils of the same type of chernozem from the Volnovaha–Mariupol region of Ukraine belonging to the Priazovska northern-steppe province (Arkhangielskij 1998). The region was chosen because it comprises the heavily polluted industrial area of the city of Mariupol and its surroundings and the unpolluted Homutovsky steppe area situated approximately 80 km to the east of Mariupol. The main goal was to determine the differences in magnetic characteristics between polluted and unpolluted soils and to relate them to the sources and extent of anthropogenic input. The city of Mariupol lies in the Donetskij region at the Priazovska coastal plane and its population reaches approximately 530 000. It is a large centre of ferrous metallurgy and mechanical engineering (Gadgi 1995). More than 50 industrial enterprises are located in a relatively small area, including two metallurgical giants (Azovstal and Illicha), a mechanical engineering plant, pipe plants, coke and graphite plants as well as other minor factories (fish cannery, dairy, etc.), the sea port and an important railroad station. Heavy smoke emissions from these enterprises as well as dust from numerous heaps of industrial waste form a dark–violet, badly smelling smoke screen above the city, containing harmful impurities in concentrations that many times exceed permissible levels. The domination of east and northeast winds with an average velocity of 4 to 6 m s^{-1} spread the contamination to the west of Mariupol. Periods with temperature inversion and cyclone weather cause most of the industrial and transport pollutants to be dispersed in the atmosphere in the near-ground level of the air. Under the influence of environmental

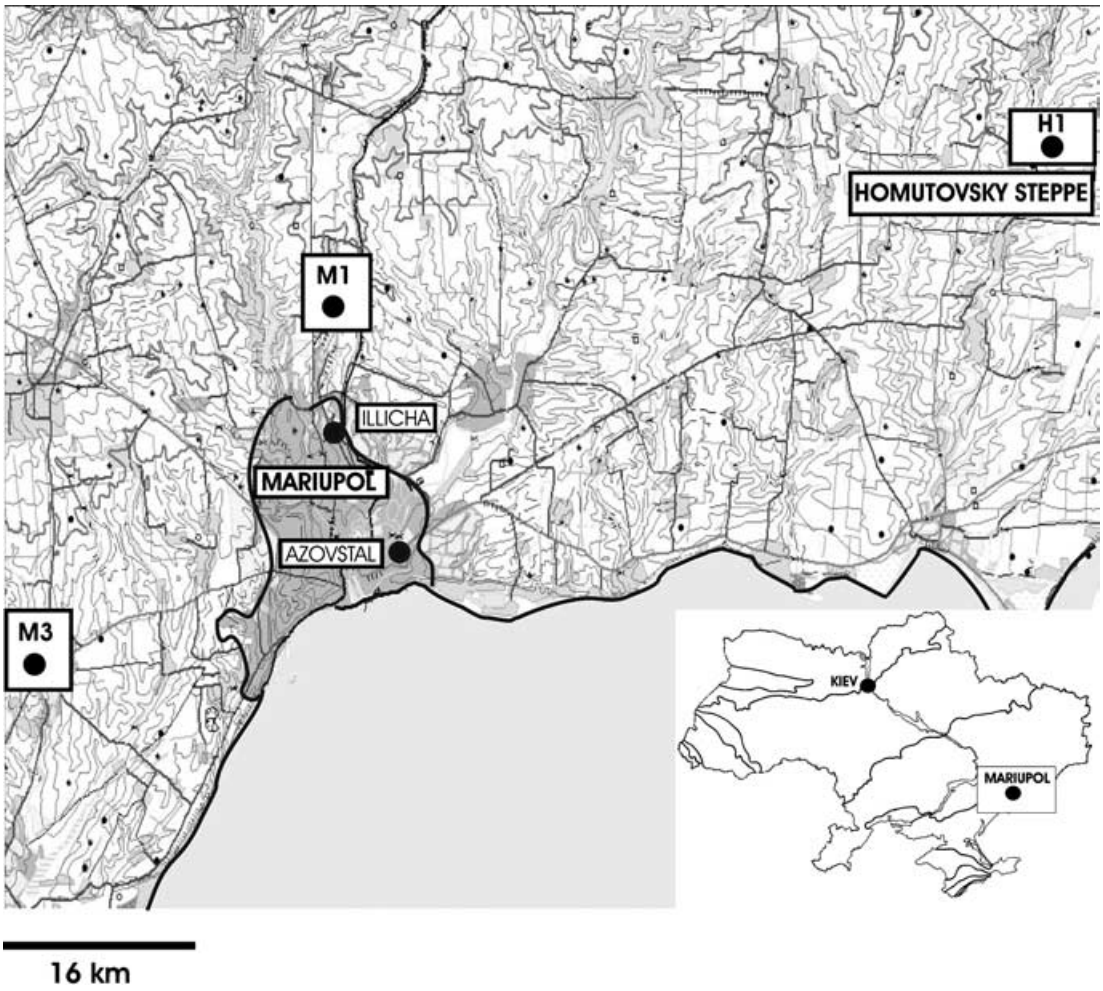

Figure 1. Map of the sampling area. Inset: map of Ukraine.

processes, a new type of soil affected by pollutants is generated. The Homutovsky steppe situated 20 km from the northern coast of the Azov sea (Fig. 1) occupies an area of 1030.4 ha. The absence of pollution and an undisturbed grassland cover that has not been cultivated for more than 120 yr makes the Homutovsky steppe representative of the typical features of a steppe zone.

2 CHARACTERISTICS OF SOIL PROFILES

The present study concerns three profiles (locations shown in Fig. 1.) taken from chernozem soil characteristic for the steppe zone of Ukraine.

(i) Two profiles from the polluted area of Mariupol: the sparsely sampled M1 profile of 1.3-m depth, situated *ca* 3 km to the north of the city, and profile M3 of 0.9-m depth sampled more densely, situated *ca* 20 km to the west of the city.

(ii) One 2-m deep profile from the unpolluted virgin chernozem of the Homutovsky steppe (H1).

Ukrainian chernozem is unique (Krupskoj & Polupan 1979). Under the steppe plants, mild and damp climatic conditions and rapid evaporation of precipitation form chernozem of characteristic dark colour, which is rich in organic matter in the form of humus. Rapid growth of tall grass encourages large organic input in the form of leaf and root decay. Light rainfall and high rates of evaporation result in only a mild degree of leaching so the upper horizons are neutral or slightly basic, rich in the nutrients Ca, Mg, Na and K that are present in all horizons. The activity of earthworms and other fauna results in excellent fine granular structure and good water-holding capacity. The upward movement of moisture in the summer causes calcium carbonate to be deposited in the form of nodules in the upper C-horizon.

The profile H1 represents ordinary chernozem that is characterized by low humus content (4–6 per cent), low thickness of humus layer (45–65 cm), carbonate appearance from a depth of 50–60 cm and slightly basic reaction. Its pedogenic division with horizons marked according to the Food and Agriculture Organization (FAO) Table (1987) is shown in Fig. 2. The same figure presents soil samples taken from the H1, M1 and M3 profiles at respective depths. Table 1 summarizes pedogenic characteristics of the profile H1.

3 MAGNETIC PROPERTIES OF THE PROFILES

3.1 Magnetic mineralogy

Magnetic mineralogy was determined by thermomagnetic experiments such as continuous thermal demagnetization of saturation isothermal remanence (SIRM) and monitoring of volume specific

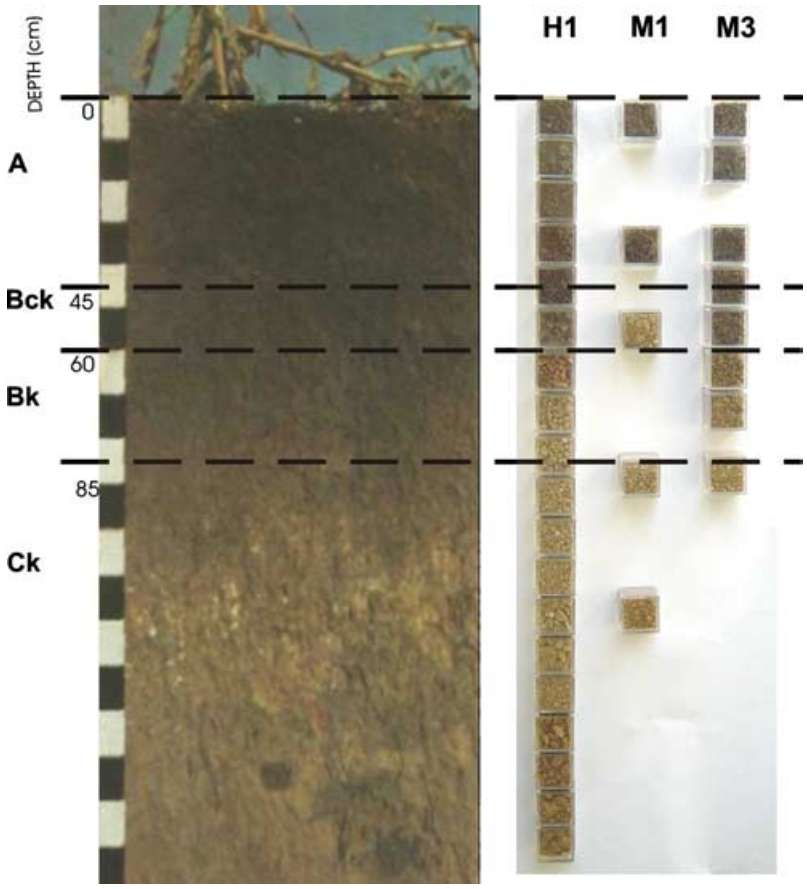

Figure 2. Example of the chernozem profile from southeast Ukraine together with sampled profiles.

Table 1. Pedogenic characteristics of soil from the profile H1.

Depth of sampling (m)	0–20	30–40	60–70	90–100	130–140	190–200
pH	7.2	7.3	7.7	7.7	7.8	7.8
$CaCO_3$	absent	absent	14.1	12.0	17.3	14.3
Grain fractions in per cent per dry non-carbonate matter						
0.01–1 mm	37.12	31.82	31.47	31.96	31.65	A 30.54
0.001–0.01 mm	20.6	18.5	17.9	20.2	18.5	20.1
<0.001 mm	40.3	38.9	36.8	33.4	31.3	32.2
Total humus	4.7	3.2	2.0	1.4	0.5	0.4

susceptibility (K) changes during heating. The SIRM decay curves provide the blocking temperature (T_b) spectra of magnetic minerals. Variations of susceptibility with temperature provide the Curie temperature and also inform us about the chemical and structural transformations taking place during heating.

SIRM thermal demagnetization was carried out with the use of a device made by TUSK enterprise from Poland. SIRM was imparted on a sample in a field of 4 T. SIRM was then measured during heating of a sample to 700 °C in magnetic screen. The temperature at which SIRM was completely demagnetized was accepted as the blocking temperature (T_b). The magnetic susceptibility χ was measured by means of the KLY-2 Czech kappabridge made by AGICO (Brno, Czech Republic) and the changes of K during heating were measured by means of the KLY-3 kappabridge. Heating was performed in air.

Thermal demagnetization of SIRM was measured for all samples along the profiles whereas K(T) curves were made for selected horizons.

3.1.1 Homutovsky steppe (H1)

Fig. 3 shows examples of the decay curves of SIRM during heating for the uppermost part of the A horizon (topsoil 0–10 cm), for the transition horizons (depths 60–70 and 70–80 cm) and for the loess (120–130 cm). Maghemite is suspected from the shape of the curves and blocking temperature slightly exceeding 600 °C for the topsoil (Fig. 3a). T_b increases with depth, reaching 670 °C in the loess horizon (Fig. 3d). This could be evidence of haematite or maghemite. From a depth of 70–80 cm, a bend around 200 °C is

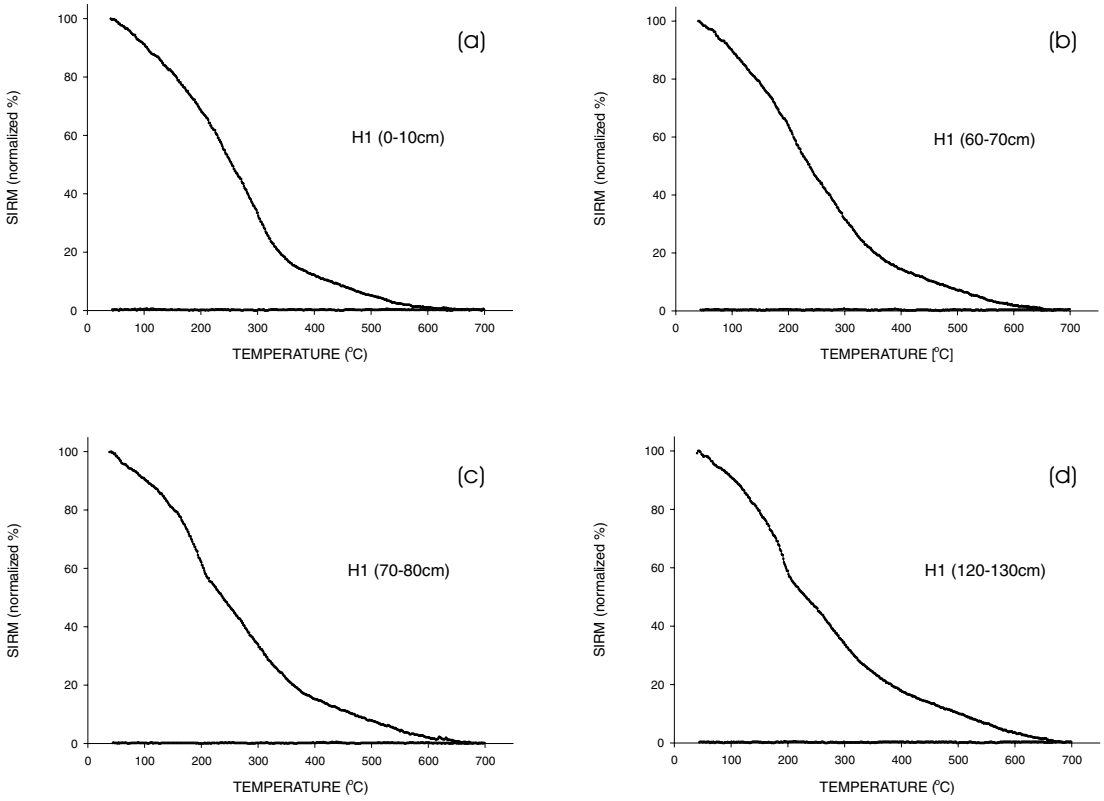

Figure 3. Examples of SIRM (T) decay curves for H1 profile: (a) sample from topsoil; (b) and (c) samples from transition zone; (d) sample from loess.

observed (Fig. 3c). The bend can be related to the presence of either maghemite or fine-grained pyrrhotite (Dekkers 1988).

The curves of susceptibility changes K(T) during continuous heating (Fig. 4) show a clear Curie point near 580 °C, the temperature characteristic for magnetite. On cooling the increase of susceptibility is observed. At room temperature the increase is 3.4 times for the sample from the topsoil (Fig. 4a) and 63 times for the sample from the loess (Fig. 4e). As the magnetite is not observed on the SIRM decay curves, its evidence on the K(T) curves should be the result of production of magnetite during heating. The K(T) curves are similar for all samples along the profile up to 450 °C. For this temperature range (Figs 4b, c, d and f), we observe a slight increase of susceptibility up to 250 °C, followed by a significant decrease up to 450 °C. At temperatures higher than 450 °C, the behaviour of K depends on depth. A big maximum at 500 °C and a dramatic drop to noise level near 580 °C was observed for all the horizons except the loess. For the loess, the maximum at 500 °C is hardly visible and the haematite tail appears. We consider the decrease of K in the range 250–450 °C to be related to the presence of maghemite, which partly converts to haematite. The maximum of K at 500 °C could be explained by growth of magnetite, however the increase of susceptibility during heating is greatest in the loess samples where the maximum is not observed. Therefore we suggest that the maximum is a demonstration of the Hopkinson effect of maghemite grains (Hrouda 1994; Hrouda *et al.* 1997). According to Dunlop (1974), we can expect a rather narrow and not very high Hopkinson peak just below the Curie point for multidomain (MD) grains, whereas the single-domain (SD) grains have a broad Hopkinson peak and a greater increase of K than MD grains. It is not clear how to classify the observed Hopkinson peaks. It is difficult to say why it is no longer observed at the base of the profile.

3.1.2 Mariupol M1

Figs 5(a), (b) and (c) show the decay curves of SIRM during heating for the topsoil (0–10 cm), the transition level (60–70 cm) and the loess (120–130 cm). The topsoil (Fig. 5a) contains magnetite and haematite seen on the SIRM (T) curve as a small tail. Magnetite is recognized down to 40 cm. Starting from this depth, the SIRM(T) curves are similar to those for H1 (Figs 5b and c). The variation of susceptibility during continuous heating for the topsoil shows the presence of magnetite (Fig. 6a). For layers deeper than 40 cm down to the bottom (Figs 6b and c), the K(T) curves are similar to those for the H1 profile. We concluded that the magnetic mineralogy of both profiles is similar with the exception of the soil between 0 and 40–50 cm where the polluted Mariupol profile contains magnetite.

3.1.3 Mariupol M3

Magnetic mineralogy of the M3 profile is between that of the M1 and H1. The presence of magnetite is seen only in the very top of the profile. This is related to the position of M3, which is situated farther from the pollution centre than the profile M1.

3.2 pARM acquisition curves

Jackson *et al.* (1988) showed that intensity of partial anhysteretic remanent magnetization (pARM) strongly depends on grain size and could be a useful tool in magnetic granulometry. They demonstrated the pARM acquisition curves for synthetic magnetite with various discrete grain size. The curves show that a maximum of intensity occurred at higher alternating field windows for finer grains. We tried to apply the pARM for determination of grain size of magnetic

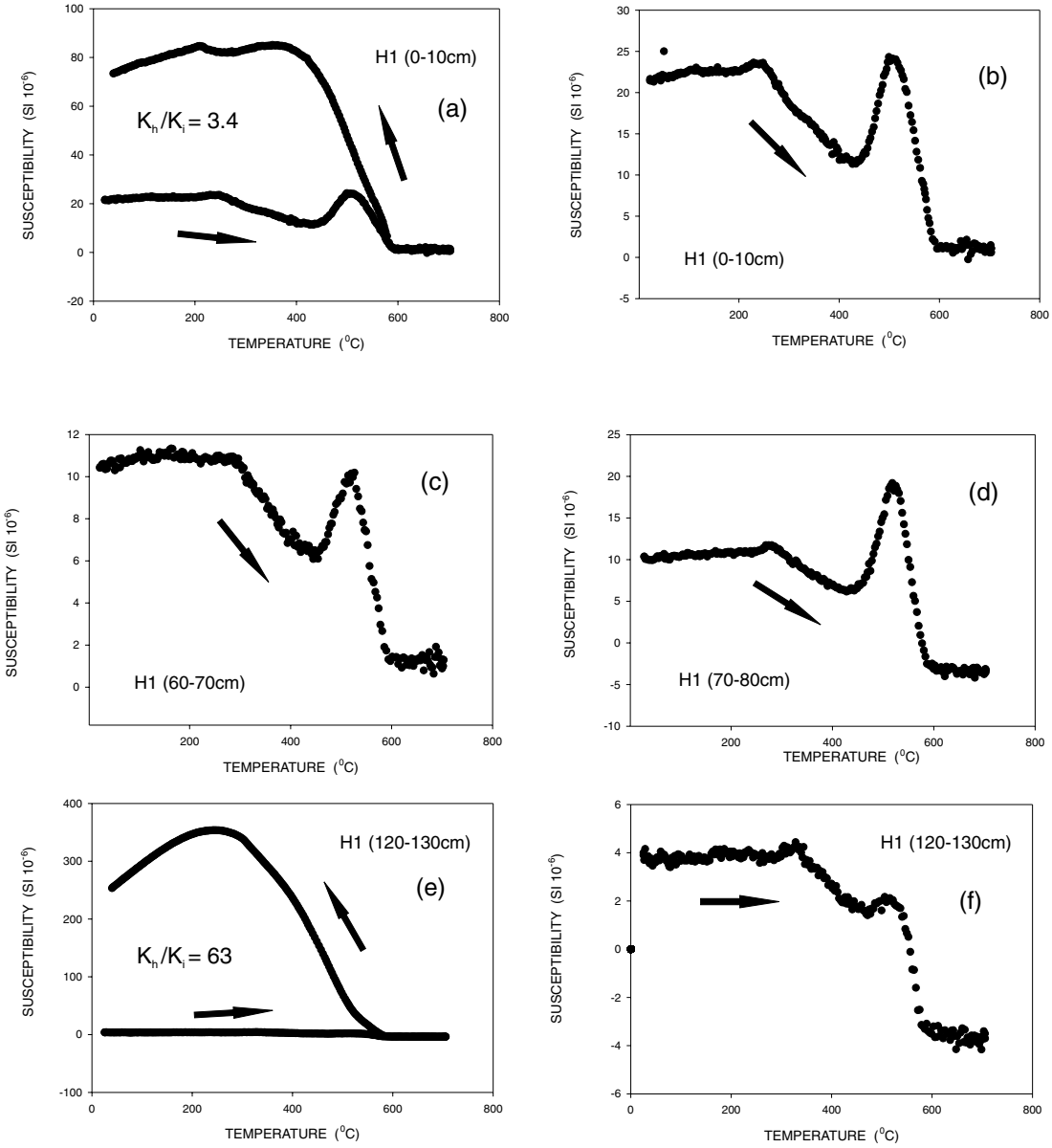

Figure 4. Changes of magnetic susceptibility during continuous heating for the H1 profile: (a) heating and cooling curves for sample from topsoil; (b) heating curve from (a); (c) and (d) heating curves for samples from transition zone; (e) heating and cooling curves for sample from loess; (f) heating curve from (e). K_i is initial susceptibility; K_h is susceptibility after heating—cooling cycle.

minerals in our soil profiles. Partial ARM was produced by subjecting a sample to an alternating field of strength H_1 and a steady field of 100 μT and then demagnetizing the generated ARM by an alternating field of H_2 strength, when $H_1 - H_2 = 10$ or 20 mT. A pARM curve was obtained by moving the window towards high alternating fields.

For the H1 profile, the curves of pARM acquisition (Fig. 7a) for the samples taken from the loess reveal two maxima of pARM acquired in the windows of alternating field of 20–10 and 60–40 mT. As magnetic parameters are similar for magnetite and maghemite, it seems reasonable to use the reference curve given by Jackson *et al.* (1988) for magnetite to interpret our data. According to the reference curve, the topsoil should contain the largest grains. However, ARM intensity depends also on coercivity and mineralogy (Egli & Lowrie 2002), and the contribution of haematite to ARM values, negligible in the topsoil, can become important in loess and the maxima can reflect the changes in mineralogy and coercivity, not in grain size.

For M1 and M3, the curves of pARM acquisition (Figs 7b and c) for the samples taken from the topsoil and the loess do not show significant differences.

3.3 Mössbauer measurements

Mössbauer spectra allow us to distinguish maghemite from magnetite and haematite. The samples were used in the Mössbauer measurements as absorbers in the transmission geometry. Measurements were performed at room temperature and liquid nitrogen temperature using a conventional constant acceleration spectrometer. The ^{57}Co in Rh source was used. The isomer shifts (δ) were related to the α-Fe standard.

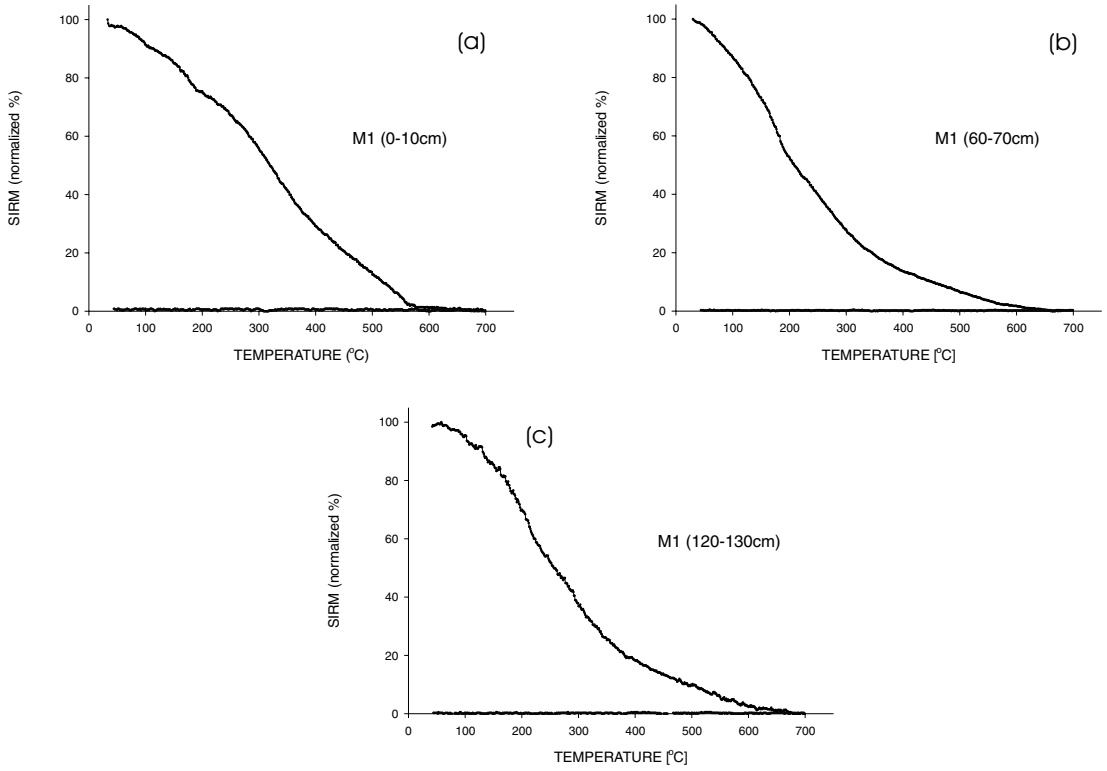

Figure 5. Examples of SIRM (T) decay curves for the M1 profile: (a) sample from topsoil; (b) sample from transition zone; (c) sample from loess.

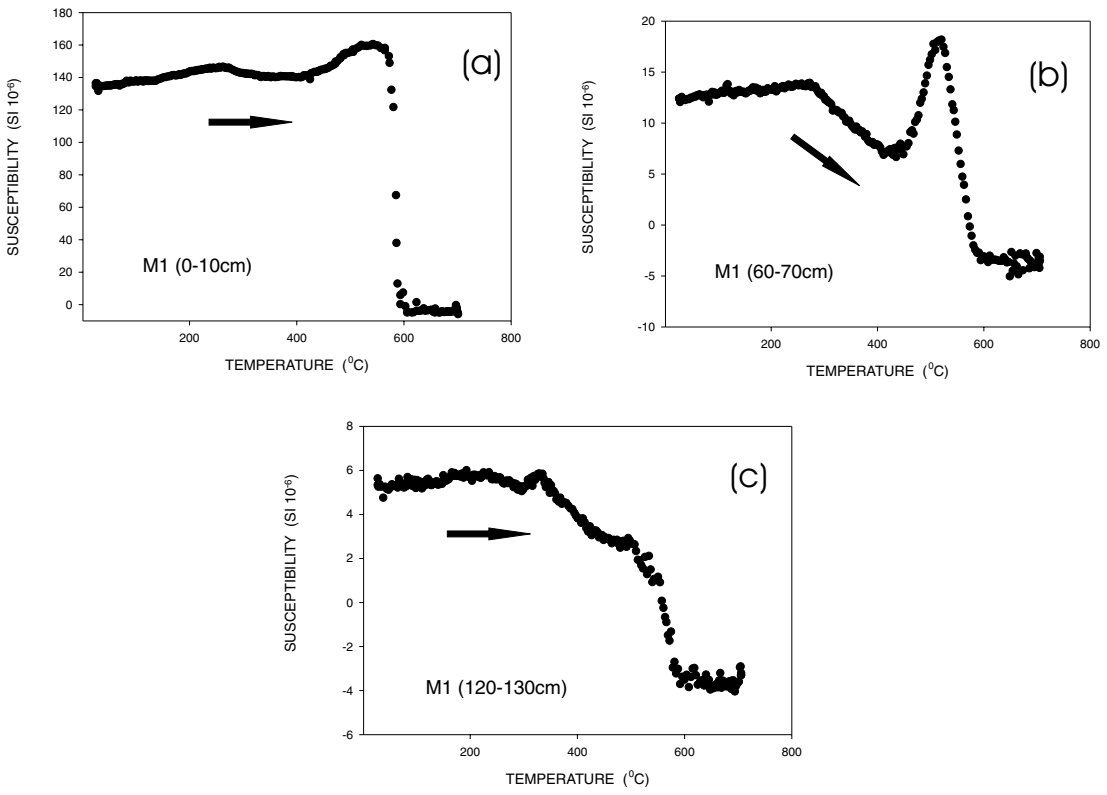

Figure 6. Changes of magnetic susceptibility during continuous heating for M1 profile. Heating curves for: (a) sample from topsoil; (b) sample from transition zone; (c) sample from loess.

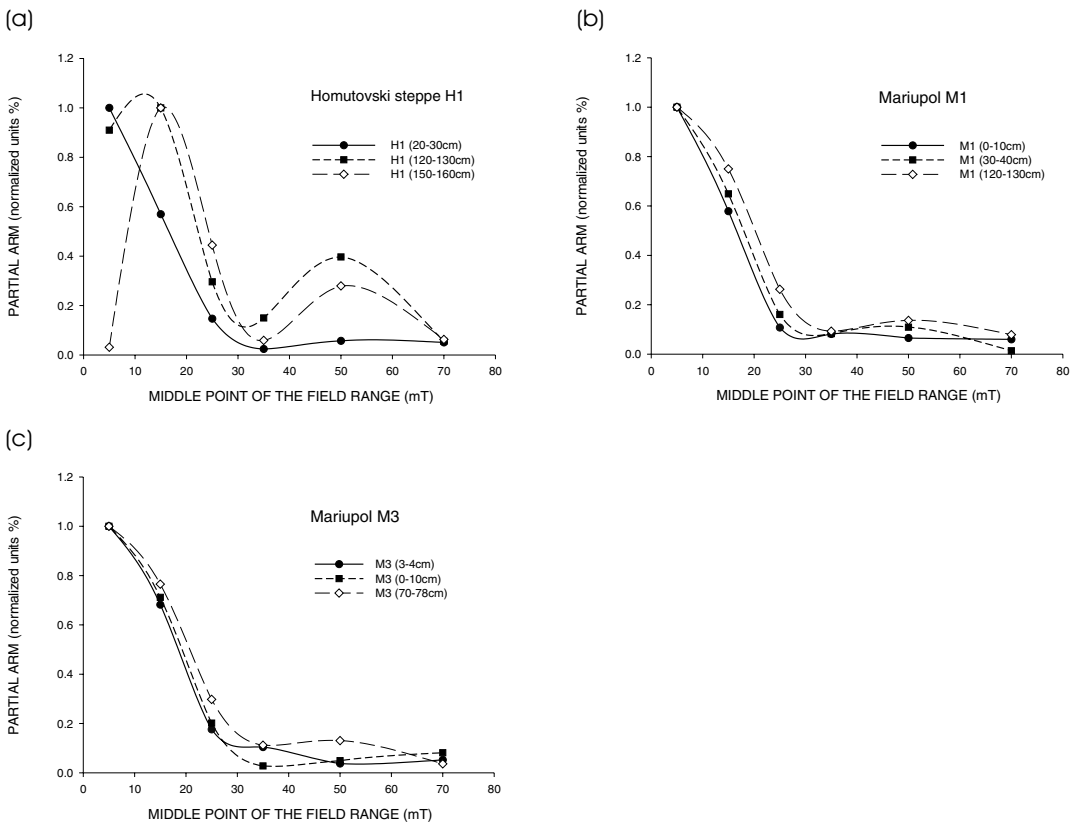

Figure 7. Examples of pARM acquisition curves for H1, M1 and M3: until 40 mT pARM was acquired in an alternating field range of 10 mT; then the range was enlarged to 20 mT.

The Mössbauer spectra were recorded for samples H1(0–10 cm), H1(120–130 cm), M1(0–10 cm), M1(30–40 cm), M1(120–130 cm) and M3(0–1 cm). The Mössbauer parameters for all subspectra are summarized in Tables 2 and 3. Figs 8 and 9 show the spectra recorded for topsoil for sampling sites H1, M1 and M3. The Mössbauer spectra measured at room temperature were fitted with three quadrupole doublets and three or four magnetic sextets. The paramagnetic doublets may originate from the following sources: (i) Fe^{3+} and Fe^{2+} cations in silicate minerals, (ii) Fe^{3+} in oxyhydroxides (β-FeOOH and γ-FeOOH) and/or (iii) from iron-containing compounds in the form of ultra fine particles in the superparamagnetic state (Kopcewicz & Kopcewicz 1999, 2001). In order to verify the origin of the quadrupole doublets, the measurements were performed at 80 K. Fig. 8 shows the Mössbauer spectra recorded at room and liquid nitrogen temperatures for sample H1(0–10 cm). The Mössbauer parameters for the spectra are collected in Table 3. The contribution of the magnetically split spectral components gradually increases as temperature decreases, at the expense of the intensity of the quadrupole doublets. Three additional sextets that appeared at low temperature reveal the hyperfine fields $B_1 = 49$ T, $B_2 = 47$ T and $B_3 = 43$ T, which permit the identification of this phase as β-FeOOH (Bowen *et al.* 1993). Taking into account the transformation of the quadrupole doublets at room temperature to magnetic sextets at low temperature, corresponding to β-FeOOH, it can be inferred that approximately 25 per cent of the spectral area of the quadrupole doublet, QS_1, with $\delta = 0.36$ mm s^{-1} and $\Delta = 0.43$ mm s^{-1}, and approximately 17 per cent of the spectral area of the second quadrupole doublet, QS_2, with $\delta = 0.37$ mm s^{-1} and $\Delta = 0.93$ mm s^{-1}, correspond to β-FeOOH. The rest of the Fe^{3+} ions are probably in the form of other Fe^{3+}-bearing minerals such as ferrihydrite (QS_1 and QS_2), γ-FeOOH (QS_1), FeS_2 (pyrite) or/and silicate minerals (QS_1) and layer silicate minerals (QS_2; Goodman 1980). Additionally, the decrease of the intensity of quadrupole doublets with decreasing temperature is accompanied by a simultaneous increase of the spectral contribution of the magnetic sextets corresponding to α-Fe_2O_3, γ-Fe_2O_3 and α-FeOOH, which means that part of these compounds appear in the form of ultra fine particles in the superparamagnetic state (Murat & Johnston 1987). The changes of the relative absorption area of the spectrum recorded at room temperature and liquid nitrogen temperature suggest that approximately 30 per cent of α-Fe_2O_3, 12 per cent of α-FeOOH but only 3 per cent of γ-Fe_2O_3 are in the superparamagnetic state.

The Mössbauer parameters obtained for all subspectra recorded at room temperature (Table 2) and the parameters obtained at 80 K (Table 3) allowed us to identify the iron-containing compounds as β-FeOOH (akaganéite) and Fe^{3+}-bearing minerals (QS_1 paramagnetic doublet), β-FeOOH and Fe^{3+}-bearing minerals (QS_2 paramagnetic doublet), Fe^{2+} silicate (QS_3 paramagnetic doublet with $\delta = 1.08$ mm s^{-1} and $\Delta = 2.74$ mm s^{-1}), and magnetically ordered compounds: α-Fe_2O_3 (haematite) and α-FeOOH (goethite) appearing in all samples. In the samples from the H1 profile, the γ-Fe_2O_3 (maghemite) and FeS_{1-x} (pyrrhotite) phases were identified. The presence of magnetic sextets corresponding to pyrrhotite suggests pyrite could also contribute to the paramagnetic part of the spectra. The Mössbauer measurements revealed the presence of Fe_3O_4 in the M1(0–10 cm) sample. The spectra show that Fe appears at

Table 2. Mössbauer parameters for selected samples (room temperature): isomer shift (δ); quadruple splitting (Δ); magnetic hyperfine field (H_{hf}).

Sample	Component	δ ($\pm$0.03) (mm s^{-1})	Δ ($\pm$0.03) (mm s^{-1})	H_{hf} ($\pm$0.2) (T)	Relative area (per cent)
M1(0–10 cm)	Fe^{3+} silicate and β-FeOOH	0.36	0.44		36.6
	Fe^{3+} silicate and β-FeOOH	0.38	0.96		20.9
	Fe^{2+} silicate	1.08	2,75		11.0
	α-Fe_2O_3	0.37		51.8	14.0
	Fe_3O_4 (Fe^{3+})	0.29		49.4	7.4
	Fe_3O_4 (Fe^{3+} and Fe^{2+})	0.63		46.1	7.7
	α-FeOOH	0.28		38.1	2.3
M1(30–40 cm)	Fe^{3+} silicate and β-FeOOH	0.36	0.42		43
	Fe^{3+} silicate and β-FeOOH	0.38	0.94		27.6
	Fe^{2+} silicate	1.08	2.72		14.8
	α-Fe_2O_3	0.37		51.2	4.8
	Fe_3O_4 (Fe^{3+})	0.37		49.0	3.0
	Fe_3O_4 (Fe^{3+} and Fe^{2+})	0.58		45.1	2.3
	α-FeOOH	0.38		37.9	2.4
	FeS	0.40		31.3	2.1
M1(120–130 cm)	Fe^{3+} silicate and β-FeOOH	0.36	0.43		43.6
	Fe^{3+} silicate and β-FeOOH	0.38	0.94		27.2
	Fe^{2+} silicate	1.08	2.72		18.5
	α-Fe_2O_3	0.34		51.5	3.6
	γ-Fe_2O_3	0.20		49.6	2.3
	α-FeOOH	0.33		37.7	1.5
	FeS	0.62		29.0	3.2
M3(0–1 cm)	Fe^{3+} silicate and β-FeOOH	0.36	0.45		50.0
	Fe^{3+} and β-FeOOH	0.37	0.98		23.8
	Fe^{2+} silicate	1.06	2.72		10.1
	α-Fe_2O_3	0.41		51.1	5.0
	Fe_3O_4 (Fe^{3+})	0.33		49.6	2.8
	Fe_3O_4 (Fe^{3+} and Fe^{2+})	0.50		45.8	3.4
	α-FeOOH	0.38		37.2	2.2
	FeS	0.47		30.0	2.7

Table 3. Mössbauer parameters for selected samples: room temperature (RT); liquid nitrogen temperature (LNT); isomer shift (δ); quadruple splitting (Δ); magnetic hyperfine field (H_{hf}).

Sample	Component	δ ($\pm$0.03) (mm s^{-1})		Δ ($\pm$).03) (mm s^{-1})		H_{hf} ($\pm$0.2) (T)		Relative area (per cent)	
		RT	LNT	RT	LNT	RT	LNT	RT	LNT
H1(0–10 cm)	Fe^{3+} silicate and β-FeOOH	0.36	0.46	0.43	0.40			45.1	34.2
	Fe^{3+} silicate and β-FeOOH	0.38	0.47	0.93	0.93			27.9	23.0
	Fe^{2+} silicate	1.08	1.2	2.74	2.89			13.2	13.1
	α-Fe_2O_3	0.32	0.51			51.4	53.5	4.3	5.6
	γ-Fe_2O_3	0.30	0.33			48.6	52.2	3.4	3.5
	α-FeOOH	0.36	0.53			37.7	50.0	3.2	3.6
	FeS	0.37	0.68			29.0	30.0	2.8	3.0
	β-FeOOH		0.48				48.1		7.0
	β-FeOOH		0.51				45.9		4.1
	β-FeOOH		0.55				43.1		2.9
H1(120–130 cm)	Fe^{3+} silicate and β-FeOOH	0.36		0.43				44.9	
	Fe^{3+} silicate and β FeOOH	0.38		0.94				25.9	
	Fe^{2+} silicate	1.1		2.72				19.3	
	α-Fe_2 O_3	0.43				50.7		3.9	
	γ-Fe_2 O_3	0.30				48.2		2.2	
	α-FeOOH	0.26				37.8		1.8	
	FeS	0.37				31.1		2.1	

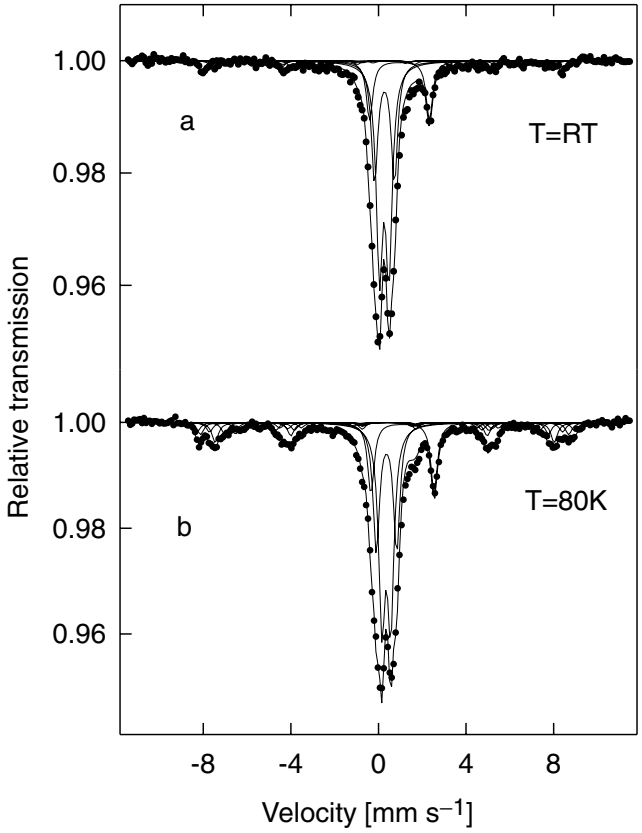

Figure 8. Mössbauer spectra for topsoil from the H1 profile measured at (a) room temperature (RT) and (b) liquid nitrogen temperature (LNT).

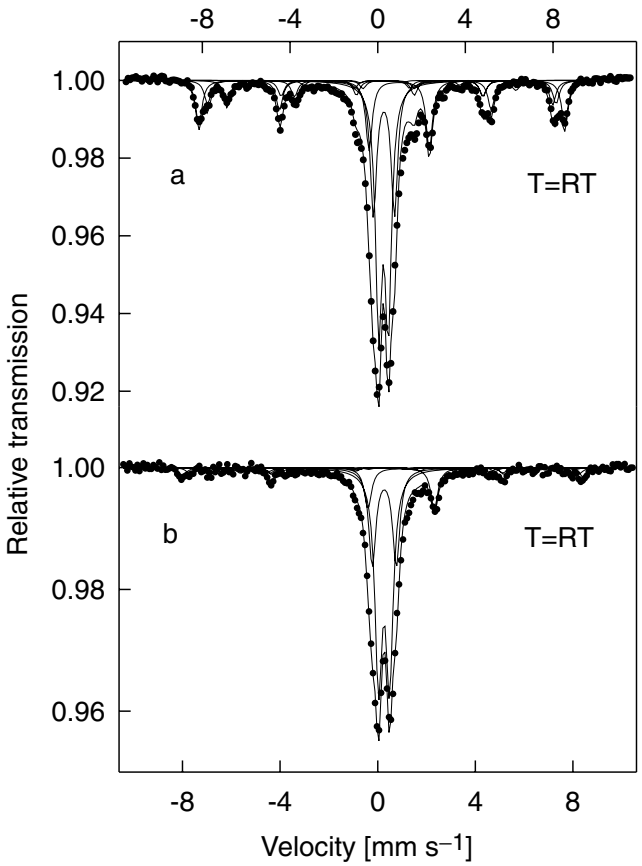

Figure 9. Mössbauer spectra for topsoil from the profiles (a) M1 and (b) M3.

two different magnetically ordered sites, corresponding to Fe^{3+} in the tetrahedral and Fe^{3+} and Fe^{2+} in the octahedral sites. For the M1(120–130 cm) sample, the maghemite and FeS_{1-x} phases were identified similarly to the case of the H1 profile. In the surface sample of the M3 profile, M3(0–1 cm), the Mössbauer spectra show the presence of haematite, magnetite and goethite as in the case of the M1 profile.

The Mössbauer measurements are in agreement with the magnetic measurements described above. The Mössbauer measurements provide useful information regarding the relative fraction of magnetic minerals occurring in particular levels of the profiles. These fractions are calculated in relation to the total Fe ions content in a given sample. As can be seen from Tables 2 and 3 for the topsoil from the M1 sampling site, the haematite and magnetite contribution to the total spectral area is approximately 14 and 15 per cent, respectively, while in the case of the loess sample (120–130 cm) the contribution of these phases to the total spectra area is considerably smaller (3.6 per cent of haematite and 2.3 per cent of maghemite fractions). For the H1 profile, these values are 4.3 per cent of haematite and 3.4 per cent of maghemite contribution for the topsoil and 3.9 and 2.2 per cent of haematite and maghemite for loess, respectively. For M3, the haematite and magnetite contribution for the topsoil is approximately 5.0 and 6.2 per cent, respectively.

3.4 Distribution of magnetic characteristics along the profiles

The following magnetic properties were measured along the profiles: mass specific susceptibility (χ); anhysteretic remanent magnetization (ARM); and the hysteresis parameters SIRM, saturation magnetization (M_s), coercivity (H_c) and coercivity of remanence (H_{cr}). Examination of the ratios: S ratio (IRM_{-100}/SIRM, where IRM_{-100} is the part of SIRM left after acquiring a back field of 100 mT), ARM_{-40}/ARM_{100} (ARM_{100} is the remanence acquired in an alternating field of 100 mT and ARM_{-40} is the part of this remanence left after demagnetizing in a field of 40 mT), ARM/χ and ARM/SIRM provides information about magnetic properties that allow to discriminate between magnetic minerals. The S ratio and ARM_{-40}/ARM_{100} are a measure of magnetic stability and are often used to estimate the contribution of soft and hard magnetic minerals. The ARM/χ ratios provide information about the shape and the squareness of the hysteresis loop. The ARM/SIRM ratio is often used to identify the presence of SD particles and is also related to magnetic interaction (Maher *et al.* 1999)).

The hysteresis loop was measured by means of the VSM device made by Molspin (Newcastle upon Tyne, UK).

Anhysteretic remanence was acquired in the Czech device LDA-3 made by AGICO (Brno, Czech Republic). The total ARM was acquired in an alternating field of 100 mT and a steady field of 100 μT.

The distributions of different magnetic parameters along the profiles are shown in Figs 10 and 11. The H_c distribution is similar for all the profiles studied: very low at the top, increasing in the transition zone between 50 and 100 cm and stabilized for the loess. H_{cr} has the same distribution in the upper part of the profile, however, the hardest minerals were found in the middle part of H1 (Figs 10b and c).

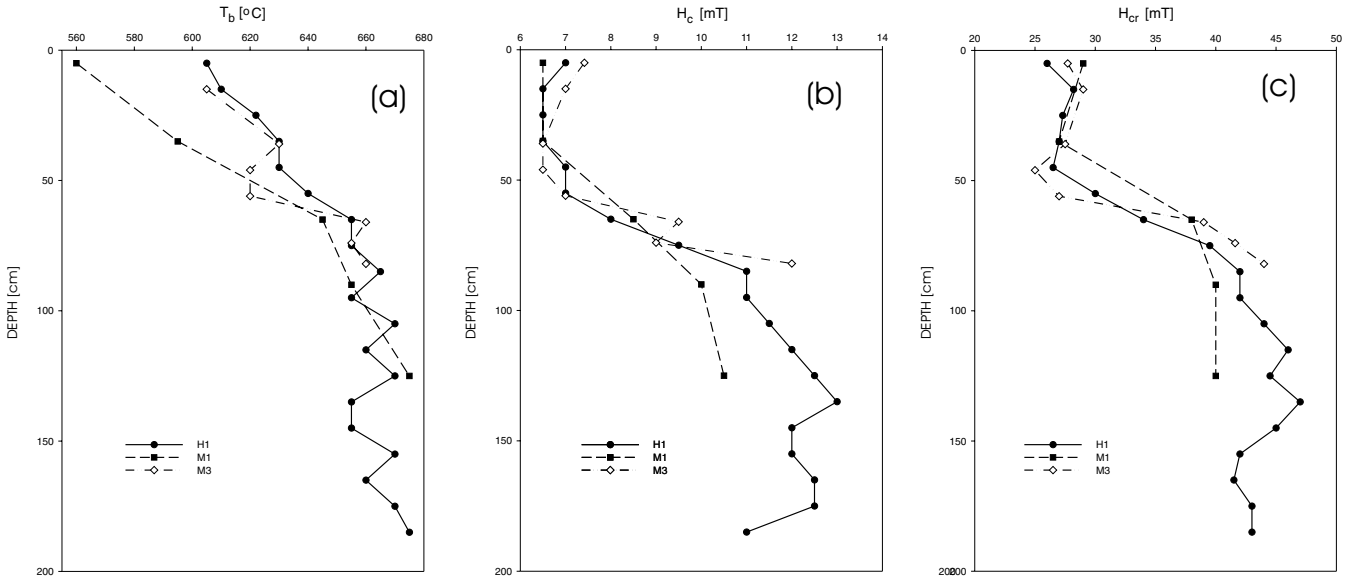

Figure 10. For the profiles H1, M1 and M3: (a) blocking temperature T_b, (b) coercivity H_c and (c) coercivity of remanence H_{cr}.

The surface value of susceptibility (Fig. 11a) at the Homutowski steppe is approximately 80×10^{-8} m^3 kg^{-1} and at Mariupol ranges from 570 to 120×10^{-8} m^3 kg^{-1} for M1 and M3, respectively. However, starting from a depth of approximately 80–100 cm, susceptibility approaches the same value of approximately 30–20 $\times$ 10^{-8} m^3 kg^{-1} for all profiles. The enhancement of χ, M_s and SIRM (Fig. 11) for polluted soil (M1) in comparison to the values for unpolluted soil (H1) is 7, 16 and 9, respectively. The relatively small increase of χ in H1 against M1 can be explained by the contribution of superparamagnetic particles in the unpolluted topsoil of the H1 profile, which resulted in relatively strong susceptibility. The presence of superparamagnetic haematite was detected by Mössbauer analysis (Table 3) in the H1 topsoil. In contrast to M_s and SIRM, the value of ARM at the top of the M1 profile is only two times greater than for H1. The relatively high value of ARM in the H1 topsoil pointed to a high contribution of fine grains in comparison to M1.

The ratio of ARM_{-40}/ARM_{100} shows consistent behaviour for all the profiles, with low values for the top horizons and a subsequent increase within the transition zone to high values in the parent material (Fig. 12a). This corresponds well to H_c behaviour (Fig. 10b) and is related to the increase of hardness of the magnetic minerals. The S ratio (IRM_{-100}/SIRM; Fig. 12b) shows a similar course as H_{cr} (Fig. 10c). The low values at the top horizons reflect the presence of maghemite or magnetite. The high values of S for the middle horizons show the increasing contribution of haematite with depth. The high values of ARM/SIRM ratio at the top of the H1 profile (Fig. 12c) indicate the presence of fine grains. The low values at the top of the M1 and M3 profiles are related to anthropogenic magnetite. The ARM/χ ratio (Fig. 12d) regarded as a measure of squareness of the hysteresis loop shows the influence of soft magnetite on the top of the M1 and M3 profiles.

4 INTERPRETATION

Identification of magnetic minerals by thermomagnetic methods revealed mainly maghemite associated with haematite in the non-polluted soil. Magnetite was identified in the polluted topsoil. Mössbauer spectra (Table 2 and 3) also identified goethite and phyrrotite. Goethite was not found by thermomagnetic experiments. Small peaks on heating curves of susceptibility at a temperature around 250–300 °C (Figs 4 and 6) can be related to phyrrotite. The SIRM(T) decay curves also show a small bend around 200 °C (Figs 3 and 5). Goethite is regarded as the most common iron oxide in a soil (Cornell & Schwertmann 2003). Haematite, often associated with goethite, points to warm and dry conditions and maturity of a soil. Although haematite was identified everywhere in all the profiles, the magnetic characteristics are related to the presence of maghemite in the non-polluted soil and magnetite in the polluted soil in the topsoil. In the loess horizon, the influence of haematite increases. Maghemite of a blocking temperature of 600–630 °C at the surface (Fig. 10a) gradually passes to maghemite of a blocking temperature of 655–675 °C in deeper levels. In the polluted soil, magnetite is observed down to 20–40 cm (A horizon). Starting from the B_{ck} and B_k horizons, magnetite is replaced by maghemite. The change of magnetic mineralogy with depth is confirmed by the distribution of the hysteresis parameters with depth (Figs 10b and c). They point to soft, strong minerals on the top (A horizon) and hard, weak mineral at the loess horizons (C_k horizon).

Variations of magnetic parameters along the profiles allowed us to identify the vertical magnetic structure of the soil, which can be compared with pedological characteristics such as pH and humus content (Maher 1986; Jordanova *et al.* 1997; Hanesch & Petersen 1999).

Three zones can be distinguished. The first zone, from the surface to a depth of 40–50 cm, corresponds to the humus layer A. In this horizon calcium carbonate is absent, the concentration of humus is between 4.7 and 3.2 per cent, and pH ranges from 7.2 to 7.3. The A horizon is characterized by high values of χ, M_s, SIRM and ARM for all the profiles. In the M1 and M3 profiles the enhancement of χ, M_s and SIRM is observed in comparison to H1. The transition zone (45–85 cm) is confined to the B_{ck} and B_k horizons and is characterized by a high value of pH, between 7.5 and 7.7, the appearance of calcium carbonate and reduction of humus concentration to approximately 2 per cent. In this zone, χ, M_s, SIRM and ARM gradually decrease to low values characteristic for the C_k horizon. The C_k horizon is characterized by lithogenic carbonate loess with pH 7.8

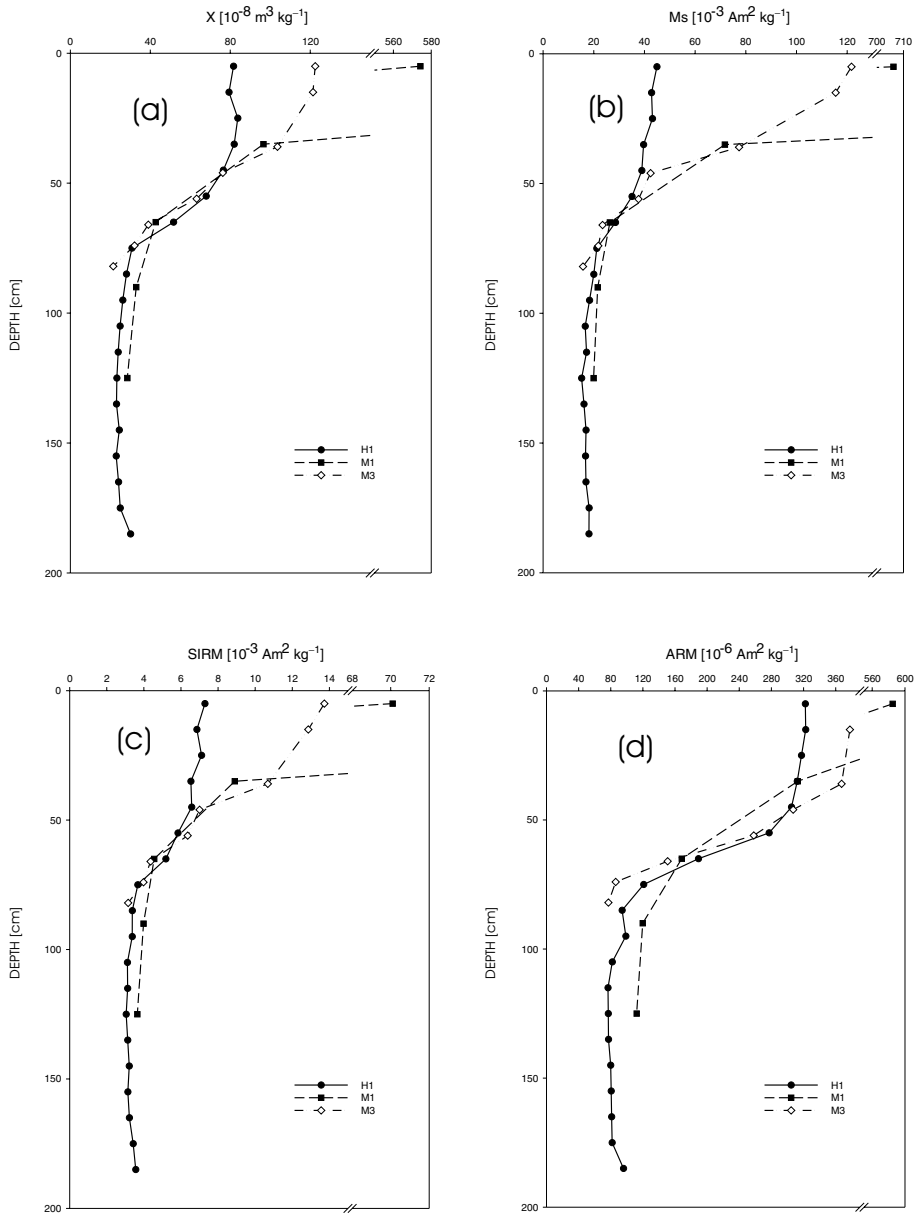

Figure 11. For the H1, M1 and M3 profiles: (a) distribution of χ, (b) M_s, (c) SIRM and (d) ARM. SIRM acquired in 1000 mT; ARM acquired in an alternating field of 100 mT and a steady field of 100 μT.

and total humus content decreasing to 0.4 per cent. For this horizon, all pedogenic and magnetic properties are stable and similar for all profiles. The differences in vertical structure for the non-polluted and polluted soils are observed mainly in the A horizon. The magnetic properties of the soil in the humus horizon A from 0 cm to a depth of 40–50 cm are related to pollution by magnetite and haematite in the case of the Mariupol area and to pedogenic processes in the Homutovski steppe.

5 CONCLUSIONS

The magnetic, vertical structure of soil profiles from Ukraine taken from non-polluted and polluted areas differs in magnetic mineralogy and distribution of magnetic minerals in the upper part of the profiles, which corresponds to the A horizon. The Mariupol profiles are polluted by magnetite and haematite. The lack of maghemite, which is present in the non-polluted profile from the Homutovsky steppe, speaks for different redox conditions within the topsoil from Mariupol. Within the transition zone, which confines the B_{ck} and B_k horizons, magnetic parameters pass to the similar magnetic characteristics of the C_k horizon for all the profiles. The pollution is lower in M3 than in M1, although the profile lies in the wind direction. This is explained by a greater distance of this profile from the city of Mariupol: the source of pollution.

ACKNOWLEDGMENTS

The authors are grateful to Professor J. Jankowski for inspiration of the Mössbauer study. This research was financially supported by the NATO Science Programme, grant no. EST.CLG.979240.

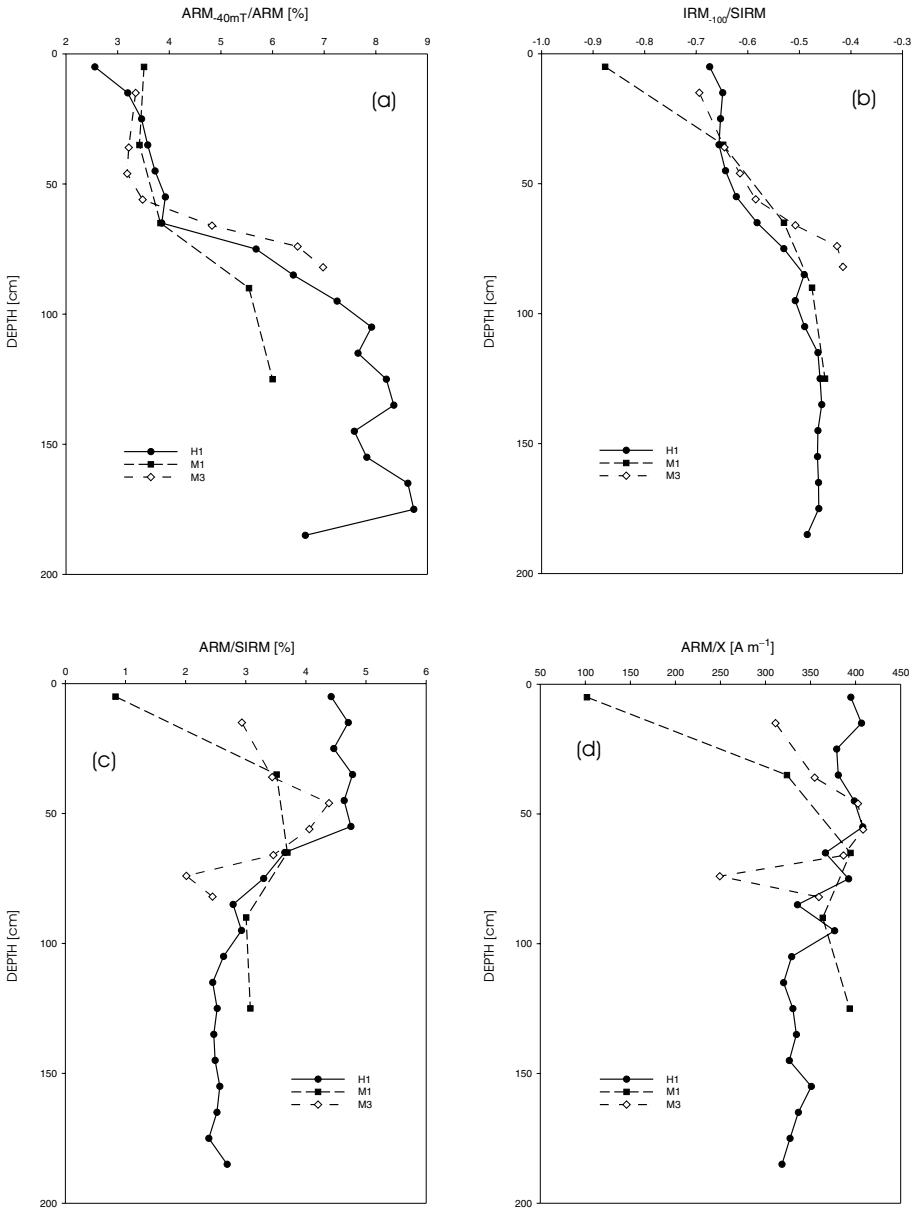

Figure 12. Distribution of the ratios for the H1, M1 and M3 profiles: (a) $ARM_{-40\,mT}/ARM$, (b) $IRM_{-100\,mT}/SIRM$, (c) SIRM/ARM and (d) ARM/χ.

REFERENCES

Arkhangielskij, I.M., 1998. Azov Sea—in oceans of problems, who should solved them, *Azov marine almanac*.

Bowen, L.H., De Grave, E. & Vandenberghe, R., 1993. Mössbauer effect studies of magnetic soils and sediments, in *Mössbauer Spectroscopy Applied to Inorganic Chemistry,* Vol. 1, pp. 115–159, eds Long, G.L. & Grandjean, F., Plenum Press, New York.

Cornell, R.M. & Schwertmann, U., 2003. *The iron oxides,* Wiley-VCH Gmbh & Co. KgaA, Weinheim.

Dekkers, M.J., 1988. Some rockmagnetic parameters for natural goethite, pyrrhotite and fine-grained hematite, *Geologica Ultraiectina,* **51,** 168–173.

Dunlop, D.J., 1974. Thermal Enhancement of Magnetic Susceptibility, *J. Geophys.,* **40,** 439–451.

Egli, R. & Lowrie, W., 2002. Anhysteretic remanent magnetization of fine magnetic particles, *J. geophys. Res.,* **107**(B10), EPM 2, 1–21.

FAO/UNESCO, 1997. *Soil Map of the World,* Technical Paper 20, ISRIC, Wageningen.

Gadgi, J.H., 1995. *Ecological problems of Mariupol and Azov Sea, Handbook*, Mariupol.

Goodman, B.A., 1980. Mössbauer spectroscopy, in *Advanced Chemical Methods for Soil and Clay Minerals Research*, pp. 1–92, eds Stucki, J.W. & Banwart, W.L., D. Reidel Publishing Company, Dordrecht.

Hanesch, M. & Petersen, N., 1999. Magnetic properties of a recent parabrown-earth from Southern Germany, *Earth planet. Sci. Lett.,* **169,** 85–97.

Hrouda, F., 1994. A technique for the measurements of thermal changes of magnetic susceptibility of weakly magnetic rocks by the CS-2 apparatus and KLY-2 Kappabridge, *Geophys. J. Int.,* **118,** 604–612.

Hrouda, F., Jelínek, V. & Zapletal, K., 1997. Refinement of the technique for susceptibility resolution into ferromagnetic and paramagnetic components, *Geophys. J. Int.,* **129,** 715–719.

Jackson, M., Gruber, W., Marvin, J. & Banerjee, S.K., 1988. Partial anhysteretic remanence and its anisotropy: applications and grain size dependence, *Geophys. Res. Lett.,* **15**(5), 440–443.

Jordanova, D., Petrovsky, E., Jordanova, N., Evlogiev, J. & Butchvarova, V., 1997. Rock magnetic properties of recent soils from northeastern Bulgaria, *Geophys. J. Int.,* **128,** 474–488.

Kopcewicz, B. & Kopcewicz, M., 1999. Mössbauer Study of the Structure of Iron-Containing Atmospheric Aerosols, in *Analytical Chemistry of Aerosols*, pp. 185–195, ed. Spurny, K.R., Lewis Publishers, Boca Raton/London/New York/Washington DC.

Kopcewicz, B. & Kopcewicz, M., 2001. Long-term measurements of iron-containing aerosols by Mössbauer spectroscopy in Poland, *Atmos. Environ.,* **35,** 3739–3747.

Krupskoj, N.K. & Polupan, N.I., 1979. *Atlas of soils of Ukrainian Republik,* Urozhay, Kyiv.

Maher, B.A., 1986. Characterisation of soil by mineral magnetic measurements, *Phys. Earth planet. Int.,* **42,** 76–92.

Maher, B.A., Thompson, R. & Hounslow, M.W., 1999. Introduction, in *Quaternary Climates, Environments and Magnetism*, pp. 1–48, eds Maher, B.A. & Thompson, R., Cambridge University Press, Cambridge.

Murat, E. & Johnston, J.H., 1987. Iron oxides and oxyhydroxides, in *Mössbauer Spectroscopy Applied to Inorganic Chemistry*, Vol. 2, pp. 507–582, eds Long, G.L. & Grandjean, F., Plenum Press, New York.

Petrovsky, E. & Ellwood, B.B., 1999. Magnetic monitoring of air-, land- and water-pollution, in *Quaternary Climates, Environments and Magnetism*, pp. 279–322, eds Maher, B.A. & Thompson, R., Cambridge University Press, Cambridge.